Inorganic Chemistry

Article

pubs.acs.org/IC

Acetylcholine-like and Trimethylglycine-like PTA (1,3,5-Triaza-7-phosphaadamantane) Derivatives for the Development of Innovative Ru- and Pt-Based Therapeutic Agents

Valeria Ferretti,[†] Marco Fogagnolo,[†] Andrea Marchi,[†] Lorenza Marvelli,[†] Fabio Sforza,[‡] and Paola Bergamini*[,†]

[†]Dipartimento di Scienze Chimiche e Farmaceutiche, Università degli Studi di Ferrara, Via Fossato di Mortara 17, 44121 Ferrara, Italy

[‡]Dipartimento di Biochimica e Biologia Molecolare, Sezione di Biologia Molecolare, Università degli Studi di Ferrara, Via Fossato di Mortara 74, 44121 Ferrara, Italy

Supporting Information

ABSTRACT: The PTA *N*-alkyl derivatives ($PTAC_2H_4OCOMe$)X (**1X**: **1a**, X = Br; **1b**, X = I; **1c**, X = PF_6; **1d**, X = BPh_4), ($PTACH_2COOEt$)X (**2X**: **2a**, X = Br; **2b**, X = Cl; **2c**, X = PF_6), and ($PTACH_2CH_2COOEt$)X (**3X**: **3a**, X = Br; **3c**, X = PF_6), presenting all the functional groups of the natural cationic compounds acetylcholine or trimethylglycine combined with a P-donor site suitable for metal ion coordination, were prepared and characterized by NMR, ESI-MS, and elemental analysis. The X-ray crystal structures of **1d** and **2c** were determined. Ligands **1c**, **2b**, and **3c** were coordinated to Pt(II) and Ru(II) to give the cationic complexes *cis*-$[PtCl_2(\mathbf{L})_2]X_2$ and $[RuCpCl(PPh_3)(\mathbf{L})]X$ (**L** = **1**, **2**, **3**, X = Cl or PF_6) designed with a structure targeted for anticancer activity. The X-ray crystal structure of $[CpRu(PPh_3)(PTAC_2H_4OCOMe)Cl]PF_6$ (**1cRu**) was determined. The antiproliferative activity of the ligands and the complexes was evaluated on three human cancer cell lines.

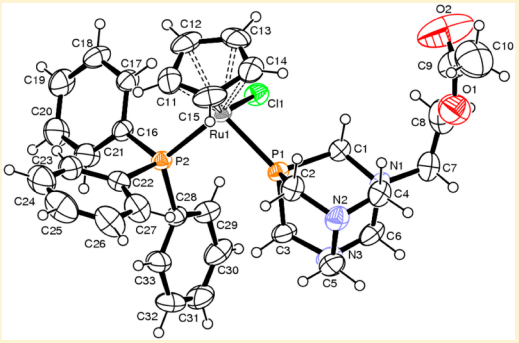

INTRODUCTION

There is still a great interest in medical applications of metal complexes. The present challenges of inorganic medicinal chemistry are (a) to improve the therapeutic performance of classic platinum anticancer drugs, based on over 30 years of research and successful clinical use,[1] and (b) to open a new scenario by investigating the potential activity of metal drugs for the diagnosis and therapy of other pathologies, mainly neurodegenerative diseases, where an aberrant biochemistry of endogenous metals seems to have a relevant role.[2] The design and synthesis of metal compounds capable of reaching the central nervous system (CNS), overcoming the physiological protecting barriers, meet both purposes. In fact traditional platinum-containing anticancer drugs do not reach therapeutic concentrations in the CNS and therefore cannot be used against brain cancer;[3] for the same reason the possibility of a positive interference of exogenous metal complexes with biochemical mechanisms causing neurodegenerative diseases has just started to get attention.[4]

Following the consolidated idea that endogenous molecules with appropriate character could bind therapeutics and drag them into specific biological cycles,[5] we looked for natural molecules suited to be introduced as ligands in Pt and Ru complexes, hopefully improving their performance related to the above-described aims. Our attention has been recently attracted by molecules bearing a quaternary ammonium group, for the following reasons:

- When inserted in a metal complex, they should favor the antiproliferative effect on cancer cells because of the electrostatic attraction between N^+ and the polyanionic DNA.
- They could exploit OCTs (organic cation transporters) expressed in the brain−blood barrier (BBB) to pass from the blood to CNS, thus acting as Trojan horses for metal ions.[6]

We describe here our work on synthetic analogues of two model molecules containing a quaternary ammonium group, acetylcholine and trimethylglycine. We designed a structural modification of their structure in order to synthesize derivatives preserving all the functional groups of the natural molecule, associated with a suitable coordination site for metals.

The work previously reported by us and others[7] about N-alkylation of PTA (1,3,5-triaza-7-phosphaadamantane) suggested that **1X**, **2X**, and **3X** could represent appropriate, readily available candidates for our purposes. In Scheme 1 the structural analogies with the natural molecules are highlighted.

Received: December 3, 2013
Published: May 6, 2014

   dx.doi.org/10.1021/ic402953s | *Inorg. Chem.* 2014, 53, 4881−4890

Scheme 1

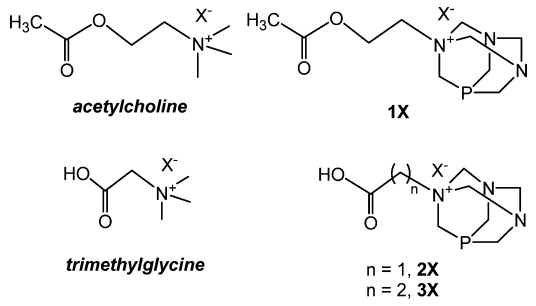

PTA and its derivatives are attracting increasing attention for medicinal applications because of their favorable properties such as stability to oxidation, small dimensions, and solubility in water.[8] A group of Ru-PTA complexes called RAPTA type are particularly promising species, mainly because of their peculiar antimetastatic activity, never observed before in other metal anticancer drugs.[9]

EXPERIMENTAL SECTION

General Procedures. All the reactions were routinely performed under a dry nitrogen atmosphere. The compound PTA[10] and the metal complex precursors *cis*-$[PtBr_2(PTA)_2]$,[11] $[CpRu(PPh_3)_2Cl]$, and $[CpRu(PPh_3)(PTA)Cl]$[12] were prepared as described in the literature. All chemicals and solvents were used as purchased (reagent grade). NMR spectra were recorded at 25 °C on a Varian Gemini 300 MHz spectrometer (^{1}H at 300 MHz, ^{13}C at 75.43 MHz, ^{31}P at 121.50 MHz) and a Varian 400 MHz (^{1}H at 400 MHz, ^{13}C at 100.57 MHz, ^{31}P at 161.92 MHz). The ^{13}C and ^{31}P spectra were run with proton decoupling, and ^{31}P spectra are reported in ppm relative to an external 85% H_3PO_4 standard, with positive shifts downfield. ^{13}C NMR spectra are reported in ppm relative to external tetramethylsilane (TMS), with positive shifts downfield. The ESI mass spectra were acquired with a Micromass LCQDuo Finningan. Elemental analyses (C, H, N) were performed using a Carlo Erba instrument model EA1110. FT-IR spectra were recorded on a Bruker Vertex 70 FT-IR instrument (4000−400 cm^{-1}).

Synthesis of (PTAC$_2$H$_4$OCOMe)Br, 1a. *Step (i): Synthesis of BrC$_2$H$_4$OCOMe.* A flask containing acetic anhydride (1.6 g, 1.5 × 10^{-2} mol) and a drop of 98% H_2SO_4 was cooled in an ice-bath; previously precooled 2-bromoethanol (1.0 g, 8 × 10^{-3} mol) was added in the same flask at 0 °C. The mixture was left at room temperature for 20 h and subsequently transferred into a separating funnel with 30 mL of diethyl ether. The organic phase was treated with a saturated aqueous solution of $NaHCO_3$ and a saturated aqueous solution of NaCl and finally was dried over anhydrous sodium sulfate. The final solution was concentrated under vacuum to a small volume, and the product was isolated as a pale yellow oil (1.2 g, 7.2 × 10^{-3} mol, yield 90%). ^{1}H NMR (400 MHz, $CDCl_3$) δ (ppm): 2.09 (s, 3H, CH_3), 3.50 (t, 2H, $^3J_{HH}$ = 6.2 Hz, BrCH_2), 4.37 (t, 2H, $^3J_{HH}$ = 6.2 Hz,−CH_2OCOMe).

Step (ii): PTA Alkylation with BrC$_2$H$_4$OCOMe. PTA (0.3 g, 1.91 × 10^{-3} mol) was dissolved in acetone (30 mL), and the mixture was gently warmed; an excess of BrC_2H_4OCOMe (1.59 g, 5 equiv) was added to the solution, and the mixture was stirred under reflux for 3 h. **1a** precipitated as an off-white solid. The warm mixture was filtered, and the isolated solid product was dried under vacuum (0.48 g, 1.48 × 10^{-3} mol, yield 78%). Anal. Calcd for $C_{10}H_{19}BrN_3O_2P$ (MW 324): C 37.0, H 5.9, N 13.0. Found: C 37.1, H 5.9, N 12.7. IR: CO 1746 cm^{-1}. ^{31}P{^{1}H} NMR (121.5 MHz, d_6-dmso) δ (ppm): −84.77 (s). ^{1}H NMR (300 MHz, d_6-dmso) δ (ppm): 2.05 (s, 3H, OCOCH_3), 3.20 (m, 2H, N$^+CH_2$CH$_2$OCOCH$_3$), 3.91 (m, 4H, NCH_2P), 4.41 (m, 2H, N$^+$CH$_2$$CH_2$OCOCH$_3$), 4.49 (m, 2H, NCH$_2$N), 4.74 (m, 2H, N$^+CH_2$P), 4.98 (m, 2H, N$^+CH_2$N), 5.10 (m, 2H, N$^+CH_2$N). ^{13}C{^{1}H} NMR (100.57 MHz, d_6-dmso) δ (ppm): 20.8 (CH_3), 45.2 (d, $^1J_{PC}$ = 19.9 Hz, 2C, NCH$_2$P), 52.1 (d, $^1J_{PC}$ = 32.1 Hz, 1C, N$^+$CH$_2$P), 56.0 (1C, N$^+CH_2$CH$_2$CO), 60.0 (1C, N$^+$CH$_2$$CH_2$CO), 70.5 (1C, NCH$_2$N), 79.1 (2C, NCH$_2N^+$), 169.9 (1C, CO). ESI-MS: observed *m*/*z* 244, calculated 244 for $C_{10}H_{19}N_3O_2P$ [M − Br]$^+$. $S_{25\ °C}$ (H_2O): 700 g L^{-1}.

Synthesis of (PTAC$_2$H$_4$OCOMe)I, 1b. *Step (i): Synthesis of IC$_2$H$_4$OCOMe.* $IC_2H_4OCOCH_3$ was obtained as a pale yellow oil through the same procedure above-described for BrC_2H_4OCOMe, using 2-iodoethanol (1.0 g, 5.8 × 10^{-3} mol) and acetic anhydride (1.2 g, 1.2 × 10^{-2} mol, 2 equiv). ^{1}H NMR (400 MHz, $CDCl_3$) δ (ppm): 2.09 (s, 3H, CH_3), 3.30 (t, $^3J_{HH}$ = 6.0 Hz, 2H, ICH_2), 4.33 (t, $^3J_{HH}$ = 6.0 Hz, 2H, −CH_2OCOMe) ppm.

Step (ii): PTA Alkylation with IC$_2$H$_4$OCOMe. PTA (0.062 g, 4 × 10^{-4} mol) was dissolved in acetone (30 mL), and the mixture was gently warmed; an excess of IC_2H_4OCOMe (0.17 g, 8 × 10^{-4} mol) was then added to the solution, and the mixture was refluxed for 15 min. The pale yellow solid (PTAC$_2$H$_4$OCOCH$_3$)I was filtered off, washed with diethyl ether, and dried under vacuum. (0.06 g, 2.47 × 10^{-4} mol, yield 62%). Anal. Calcd for $C_{10}H_{19}I\ N_3O_2P$ (MW 371): C 32.4, H 5.2, N 11.3. Found: C 32.5, H 5.4, N 11.1. IR: CO 1746 cm^{-1}. ^{31}P{^{1}H} NMR (121.5 MHz, d_6-dmso) δ (ppm): −83.67. ^{1}H NMR (300 MHz, d_6-dmso) δ (ppm): 2.05 (s, 3H, OCOCH_3), 3.15 (m, 2H, N$^+CH_2$CH$_2$OCOCH$_3$), 3.85 (m, 4H, NCH_2P), 4.40 (m, 2H, PCH_2N$^+$ + 2H, CH_2OCOCH$_3$), δ 4.47 (d, 2H, CH_2, NCH_2N), 4.90 (m, 2H, CH_2, NCH$_2$N$^+$), 5.10 (m, 2H, N$^+$CH$_2$N). $S_{25\ °C}$ (H_2O): 270 g L^{-1}.

Synthesis of (PTAC$_2$H$_4$OCOMe)PF$_6$, 1c. A methanolic solution of KPF_6 (0.17 g, 0.93 × 10^{-3} mol, 1.5 equiv) in 1 mL of MeOH was added dropwise to a solution of (PTAC$_2$H$_4$OCOMe)Br (0.2 g, 0.62 × 10^{-3} mol) in the same solvent (40 mL). The solvent was slowly evaporated in a stream of nitrogen, and microcrystals of the PF_6^- salt were filtered off, rapidly washed with methanol, and finally dried under vacuum (1.43 g, 0.37 × 10^{-3} mol, yield 60%). Anal. Calcd for $C_{10}H_{19}F_6N_3O_2P_2$ (MW 389): C 30.8, H 4.9, N 10.8. Found: C 30.5, H 5.2, N 10.5. IR: CO 1746 cm^{-1}. ^{31}P{^{1}H} NMR (121.5 MHz, D_2O) δ (ppm): −83.33 (s), −142.7 (sept, $^1J_{FP}$ = 707 Hz). ^{1}H NMR (300 MHz, D_2O) δ (ppm): 1.99 (s, 3H, OCOCH$_3$), 3.18 (m, 2H, N$^+CH_2$CH$_2$OCOCH$_3$), 3.80 (m, 4H, NCH_2P), 4.40 (m, 2H NCH$_2$N +2H N$^+CH_2$P + 2H N$^+$CH$_2$$CH_2$OCOCH$_3$), 4.98 (m, 4H, N$^+CH_2$N). ^{13}C{^{1}H} NMR (100.57 MHz, d_6-dmso) δ (ppm): 21.1 (CH_3), 45.2 (d, $^1J_{PC}$ = 20 Hz, 2C, NCH$_2$P), 51.8 (d, $^1J_{PC}$ = 32.0 Hz, 1C, N$^+$CH$_2$P), 56.0 (1C, N$^+CH_2$CH$_2$CO), 60.1 (1C, N$^+$CH$_2$$CH_2$CO), 70.7 (1C, NCH$_2$N), 79.0 (2C, NCH$_2N^+$), 170.0 (1C, CO). $S_{25\ °C}$ (H_2O): 0.74 g L^{-1}.

Synthesis of (PTAC$_2$H$_4$OCOMe)BPh$_4$, 1d. A solution of $NaBPh_4$ (0.3 g, 3.3 × 10^{-4} mol, 1.1 equiv) in MeOH (3 mL) was added to a solution of (PTAC$_2$H$_4$OCOMe)Br (0.1 g, 3 × 10^{-4} mol) in 20 mL of MeOH. **1d** precipitated as white microcrystals, which were filtered off and washed with diethyl ether (0.09 g, 1.52 × 10^{-4} mol, yield 51%). The crude product was recrystallized at room temperature from acetone and diethyl ether, giving crystals suitable for X-ray analysis (see Figure 1 and Table 2). ^{31}P{^{1}H} NMR (121.5 MHz, d_6-dmso) δ (ppm): −84.66 (s). ^{1}H NMR (300 MHz, d_6-dmso) δ (ppm): 2.00 (s, 3H, OCOCH$_3$), 3.21 (m, 2H, N$^+CH_2$CH$_2$OCOCH$_3$), 3.79 (m, 4H, NCH_2P), 4.40 (m, 2H, NCH$_2$N + 2H, N$^+CH_2$P + 2H, N$^+$CH$_2$$CH_2$OCOCH$_3$), 5.00 (m, 4H, N$^+CH_2$N) ppm, 6.5−7.5 (m, 20H, Ph). $S_{25\ °C}$ (H_2O): 1.6 × 10^{-2} g L^{-1}.

Synthesis of *cis*-[(PTAC$_2$H$_4$OCOMe)$_2$PtCl$_2$](PF$_6$)$_2$, 1cPt. A solution of (PTAC$_2$H$_4$OCOMe)PF_6 (0.11 g, 2.83 × 10^{-4} mol) in H_2O (10 mL) was added to an aqueous solution of K_2PtCl_4 (0.058 g, 1.4 × 10^{-4} mol; 1 mL of H_2O) under stirring. An off-white solid immediately started to precipitate. After 4 h, the cream-white solid was collected on a sintered glass-frit, washed with water, and dried over P_2O_5 (0.06 g, 5.7 × 10^{-5} mol, yield 40%). Anal. Calcd for $C_{20}H_{38}Cl_2F_{12}N_6O_4P_4Pt$ (MW 1044): C 23.0, H 3.7, N 8.0. Found: C 22.5, H 3.8, N 7.8. IR: CO 1745 cm^{-1}. ^{31}P{^{1}H} NMR (121.5 MHz, d_6-dmso) δ (ppm): −41.74 (s, $^1J_{PtP}$ 3495 Hz), −142.7 (sept, PF_6^-, $^1J_{FP}$ = 707 Hz). ^{1}H NMR (300 MHz, d_6-dmso) δ (ppm): 2.0 (s, 3H, OCOCH$_3$), 2.7 (m, 2H, −N$^+CH_2$CH$_2$OCOMe), 4.5 (bm, 10H), 5.0−5.2 (m, 4H, N$^+$CH$_2$N). ESI-MS: observed *m*/*z* 377, calculated 377 for $C_{20}H_{38}Cl_2N_6O_4P_2Pt$ [M − 2PF_6]$^{2+}$. $S_{25\ °C}$ (H_2O): 0.01 g L^{-1}.

dx.doi.org/10.1021/ic402953s | Inorg. Chem. 2014, 53, 4881−4890

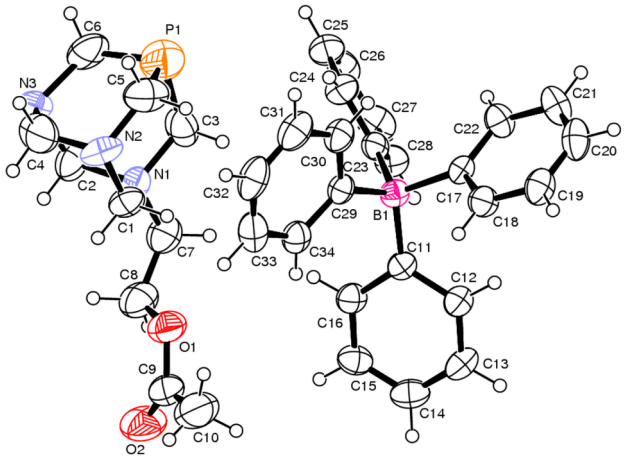

Figure 1. ORTEP view and atom-numbering scheme for **1d**. Thermal ellipsoids are drawn at the 40% probability level.

Synthesis of [CpRu(PPh$_3$)(PTAC$_2$H$_4$OCOMe)Cl]Br, 1aRu. To a solution of [CpRu(PPh$_3$)(PTA)Cl] (0.1 g, 1.6 × 10^{-4} mol) in 25 mL of acetone was added dropwise a large excess of 2-bromoethyl acetate (10 equiv). After 24 h under stirring, **1aRu** was recovered as a yellow solid, filtered off, and washed with ethyl ether (0.04 g, 4.8 × 10^{-4} mol, yield 30%). ^{31}P{^{1}H} NMR (121.5 MHz, d_6-dmso) δ (ppm): 46.45 (d, PPh$_3$, $^2J_{PP}$ = 43.7 Hz), −14.32 (d, $^2J_{PP}$ = 43.7 Hz). ^{1}H NMR (300 MHz, d_6-dmso) δ (ppm): 2.07 (s, 3H, OCOCH$_3$), 2.70 (m, 2H, −N$^+$*CH*$_2$CH$_2$OCOMe), 3.21 (m, 4H, NC*H*$_2$P), 3.45 (m, 2H, −N$^+$CH$_2$*CH*$_2$OCOMe), 4.42 (m, 4H, NCH$_2$N + N$^+$*CH*$_2$P), 4.56 (s, Cp, 5H), 4.7−5.0 (m, 4H, N$^+$CH$_2$N), 7.35−7.50 (15H, PPh$_3$).

Synthesis of [CpRu(PPh$_3$)(PTAC$_2$H$_4$OCOMe)Cl]PF$_6$, 1cRu. A slight excess of solid **1c** (0.08 g, 0.2 × 10^{-3} mol, 1.5 equiv) was added under stirring to a solution of [CpRu(PPh$_3$)$_2$Cl], (0.1 g, 0.14 × 10^{-3} mol) in acetone (30 mL). The mixture was refluxed for 3 h. The evaporation of the solvent to a small volume and the slow addition of diethyl ether gave a light yellow precipitate, which was filtered off and dried in air (0.095 g, 0.11 × 10^{-3} mol, yield 80%). Anal. Calcd for C$_{33}$H$_{39}$ClF$_6$N$_3$O$_2$P$_3$Ru (MW 853): C 46.5, H 4.6, N 4.9. Found: C 46.1, H 4.9, N 4.5. IR: CO 1748 cm^{-1}. ^{31}P{^{1}H} NMR (121.5 MHz, d_6-dmso) δ (ppm): 46.50 (d, PPh$_3$, $^2J_{PP}$ = 43.7 Hz), −14.49 (d, **1c**, $^2J_{PP}$ = 43.7 Hz), −143.25 (PF$_6^-$, $^1J_{FP}$ = 707 Hz). ^{1}H NMR (300 MHz, d_6-dmso) δ (ppm): 2.05 (s, 3H, OCOCH$_3$), 2.72 (m, 2H, −N$^+$*CH*$_2$CH$_2$OCOMe), 3.21 (m, 4H, NC*H*$_2$P), 3.43 (m, 2H, −N$^+$CH$_2$*CH*$_2$OCOMe), 4.40 (m, 4H, NCH$_2$N + N$^+$*CH*$_2$P), 4.56 (s, Cp, 5H), 4.8−5.0 (m, 4H, N$^+$CH$_2$N), 7.35−7.50 (15H, PPh$_3$). ^{13}C{^{1}H} NMR (100.57 MHz, d_6-dmso) δ (ppm): 20.7 (CH$_3$), 49.5 (d, $^1J_{PC}$ 19.9 Hz, 2C, NCH$_2$P), 51.6 (d, $^1J_{PC}$ 32.1 Hz, 1C, N$^+$CH$_2$P), 56.1 (1C, N$^+$*CH*$_2$CH$_2$CO), 59.9 (1C, N$^+$CH$_2$*CH*$_2$CO), 64.5 (1C, NCH$_2$N), 79.4 (5C, Cp), 80.9 (2C, NCH$_2$N$^+$), 128−138 (18C, Ph), 169.9 (1C, CO). ESI-MS: observed m/z 708, calculated 708 for C$_{33}$H$_{39}$ClN$_3$O$_2$P$_2$Ru (M − PF$_6$)$^+$. $S_{25\ °C}$ (H$_2$O): 0.05 g L^{-1}.

Table 2. Selected Bond Distances and Angles and Geometrical Parameters for C−H···O and C−H···π Intermolecular Interactions in 1d (Å, deg)

bond distances		bond angles	
P1−C3	1.695(6)	C3−P1−C5	97.9(2)
P1−C5	1.698(6)	C3−P1−C6	97.5(3)
P1−C6	1.708(5)	C5−P1−C6	100.9(3)
O1−C8	1.443(6)		
O1−C9	1.338(6)		
O2−C9	1.176(6)		

	intermolecular interactions[a]			
	D−H	D···A	H···A	D−H···A
C2−H2A···O2^i	0.97	3.370(6)	2.46	154
C5−H5A···(C29−C34)^i	0.97	3.23	2.92	162

[a]Centroid; symmetry code (i): x+1/2, 3/2−y, −z.

Synthesis of (PTACH$_2$COOEt)Br, 2a. A solution of PTA (0.220 g, 1.4 × 10^{-3} mol) in 30 mL of acetone was treated with ethyl bromoacetate (0.37 g, 2.2 × 10^{-3} mol, 1.6 equiv) and stirred at room temperature for 3 h. The white precipitate was filtered off and washed with acetone (0.354 g, 1.1 × 10^{-3} mol, yield 78%).^{31}P{^{1}H} NMR (121.5 MHz, d_6-dmso) δ (ppm): −84.05 (s). ^{1}H NMR (300 MHz, d_6-dmso) δ (ppm): 1.20 (t, $^3J_{HH}$ = 5 Hz, 3H, CH$_2$*CH*$_3$), 3.92 (m, 2H, N$^+$*CH*$_2$COOEt + 4H, NCH$_2$P), 4.22 (q, $^3J_{HH}$ = 5 Hz, 2H, *CH*$_2$CH$_3$), 4.41 (d, $^2J_{HH}$ = 10 Hz, 1H, NCH$_2$N), 4.52 (m, 1H, NCH$_2$N + 2H, N$^+$CH$_2$P), 4.90 (d, $^2J_{HH}$ = 9 Hz, 2H, N$^+$CH$_2$N), 5.20 (d, $^2J_{HH}$ = 9 Hz, 2H, N$^+$CH$_2$N). $S_{25\ °C}$ (H$_2$O): 625 g L^{-1}.

Synthesis of (PTACH$_2$COOEt)Cl, 2b. PTA (0.4 g, 2.6 0.10^{-3} mol) was dissolved in warm acetone (50 mL), and the solution was treated with 800 μL of ethyl chloroacetate (0.932 g, 7.6 × 10^{-3} mol, 3 equiv); the mixture was stirred at room temperature for 18 h. An off-white solid was then filtered off and washed with acetone and diethyl ether (0.44 g, 1.6 × 10^{-3} mol, yield 61%). Anal. Calcd for C$_{10}$H$_{19}$ClN$_3$O$_2$P (MW 280): C 42.9, H 6.8, N 15.0. Found: C 43.0, H 7.1, N 14.8. IR: CO 1745 cm^{-1}. ^{31}P{^{1}H} NMR (121.5 MHz, CD$_3$OD) δ (ppm): −81.03 (s). ^{1}H NMR (300 MHz, CD$_3$OD) δ (ppm): 1.32 (t, $^3J_{HH}$ = 5 Hz, 3H, CH$_2$*CH*$_3$), 3.95 (m, 4H, NCH$_2$P + 2H N$^+$CH$_2$CO), 4.32 (q, $^3J_{HH}$ = 5 Hz, 2H, *CH*$_2$CH$_3$), 4.50 (d, $^2J_{HH}$ = 11 Hz, 1 H, NCH$_2$N),

Table 1. Crystal Data and Details of Data Collection for 1d, 1cRu, and 2c

	1d	1cRu	2c
chemical formula	(C$_{10}$H$_{19}$N$_3$O$_2$P)$^+$(C$_{24}$H$_{20}$B)$^-$	(C$_{33}$H$_{39}$ClN$_3$O$_2$P$_2$Ru)$^+$(PF$_6$)$^-$	(C$_{10}$H$_{19}$N$_3$O$_2$P)$^+$(PF$_6$)$^-$
M_r	563.46	853.10	389.22
cryst syst, space group	orthorhombic, $P2_12_12_1$	triclinic, $P\bar{1}$	monoclinic, $P2_1/n$
a, b, c (Å)	9.8011(1), 10.2689(1), 29.9161(5)	9.3552(3), 14.1403(5), 14.8980(6)	9.4394(2), 10.9595(2), 16.1133(3)
α, β, γ (deg)		68.377(2), 75.999(1), 75.979(3)	103.1990(7)
V (Å^3)	3010.95(7)	1751.87(11)	1622.88(5)
Z	4	2	4
μ (mm^{-1})	0.13	0.73	0.34
cryst size (mm)	0.39 × 0.26 × 0.15	0.19 × 0.12 × 0.04	0.44 × 0.29 × 0.19
no. of measd, indep, and obsd [$I > 2\sigma(I)$] reflns	5839, 5839, 4189	12 060, 6386, 5030	6654, 3511, 2979
R_{int}	0.040	0.037	0.013
$R[F^2 > 2\sigma(F^2)]$, $wR(F^2)$, S	0.074, 0.245, 0.99	0.051, 0.154, 1.06	0.076, 0.248, 1.13
no. of reflns	5839	6386	3511
no. of params	370	443	208
no. of restraints	6	0	0
$\Delta\rho_{max}$, $\Delta\rho_{min}$ (e Å^{-3})	0.35, −0.59	0.91, −0.80	0.64, −0.47

dx.doi.org/10.1021/ic402953s | Inorg. Chem. 2014, 53, 4881−4890

4.65 (d, $^2J_{HH}$ = 11 Hz, 1H, NCH_2N), 4.67 (d, 2H, $^2J_{HP}$ = 7 Hz, N^+CH_2P), 5.10 (d, 2H, $^2J_{HH}$ = 9 Hz, N^+CH_2N), 5.39 (d, 2H, $^2J_{HH}$ = 9 Hz, N^+CH_2N). $^{13}C\{^1H\}$ NMR (100.57 MHz, d_6-dmso) δ (ppm): 13.8 (CH_3), 45.4 (d, $^1J_{PC}$ = 20.1 Hz, 2C, NCH_2P), 52.7 (d, $^1J_{PC}$ = 33.7 Hz, 1C, N^+CH_2P), 59.2 (1C, N^+CH_2CO), 62.1 (1C, CH_2CH_3), 69.1 (1C, NCH_2N), 79.6 (2C, NCH_2N^+), 162.2 (1C, COOEt). $S_{25\,°C}$ (H_2O): 910 g L^{-1}.

Synthesis of (PTACH$_2$COOEt)PF$_6$, 2c. (PTACH$_2$COOEt)PF_6 was obtained by adding a solution of KPF_6 (0.2 g, 1.4 × 10^{-3} mol, 2 equiv) in 1 mL of methanol to a solution of **2a** (0.23 g, 7.2 × 10^{-4} mol) in 20 mL of methanol.

The solution was stirred at room temperature for 10 min and then slowly concentrated under nitrogen (over about 20 h) to give white microcrystals, which were filtered off and washed with methanol (0.17 g, 4.3 × 10^{-4} mol, yield 60%). The crude product **2c**, recrystallized at room temperature from MeOH and Et_2O, gave crystals suitable for X-ray analysis (Figure 3, Table 4). Anal. Calcd for $C_{10}H_{19}F_6N_3O_2P_2$

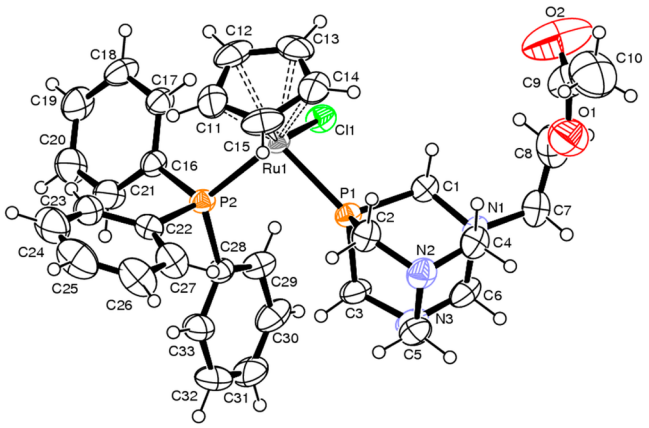

Figure 2. ORTEP view and atom-numbering scheme for **1cRu**. Thermal ellipsoids are drawn at the 40% probability level. The PF_6 anion has been omitted for clarity.

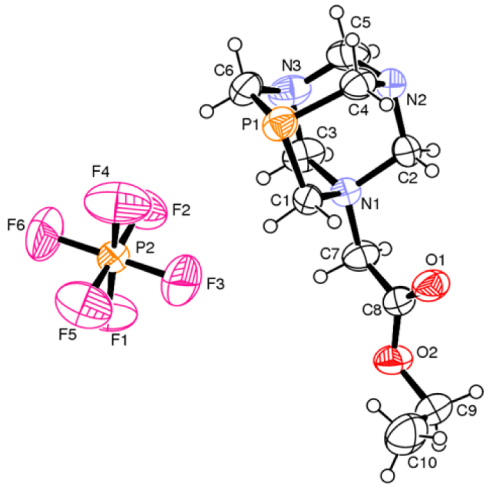

Figure 3. ORTEP view and atom-numbering scheme for **2c**. Thermal ellipsoids are drawn at the 40% probability level.

(MW 389): C 30.8, H 4.9, N 10.8. Found: C 30.8, H 4.6, N 11.0. IR: CO 1745 cm^{-1}. $^{31}P\{^1H\}$ NMR (121.5 MHz, d_6-dmso) δ (ppm): −83.46 s, −142.7 sept ($^1J_{FP}$ 707 Hz). ^1H NMR (300 MHz, CD_3OD) δ (ppm): 1.32 (t, $^3J_{HH}$ = 5 Hz, 3H, CH_3), 3.9 (m, 4H, NCH_2P+ 2H, N^+CH_2CO), 4.35 (q, $^3J_{HH}$ = 5 Hz, 2H, CH_2), 4.50 (d, $^2J_{HH}$ = 11 Hz, 1H, NCH_2N), 4.60 (d, 1H, NCH_2N), 4.67 (d, $^2J_{HP}$ = 4 Hz, 2H, N^+CH_2P), 5.05 (d, $^2J_{HH}$ = 9 Hz, 2H, N^+CH_2N), 5.35 (d, $^2J_{HH}$ = 9 Hz, 2H, N^+CH_2N). $^{13}C\{^1H\}$ NMR (100.57 MHz, CD_3OD) δ (ppm): 14.2

Table 3. Selected Bond Distances and Angles and Geometrical Parameters for C−H···Halide Intermolecular Interactions in 1cRu (Å, deg)

bond distances		bond angles	
Ru1−C1	2.455(2)	Cl1−Ru1−P1	89.63(4)
Ru1−P1	2.269(1)	Cl1−Ru1−P2	91.56(4)
Ru1−P2	2.309(1)	P1−Ru1−P2	98.20(4)
Ru1−Cp(centroid)	1.856	Cl1−Ru−Cp(centroid)	122.7
Ru−C (mean)	2.20(2)	P1−Ru−Cp(centroid)	121.3
P1−C (mean)	1.846(5)	P2−Ry−Cp(centroid)	124.7
P2−C (mean)	1.832(7)		

	intermolecular interactions[a]			
	D−H	D···A	H···A	D−H···A
C3−H···F4	0.97	3.51(1)	2.62	152
C5−H···F1	0.97	3.33(1)	2.45	152
C10−H···F6^{i}	0.96	3.25(2)	2.45	141
C5−H···F1^{ii}	0.97	3.41(1)	2.53	150
C6−H···F1^{ii}	0.97	3.424(8)	2.55	150
C6−H	0.97	3.708(6)	2.78	159
C1−H···Cl1^{iii}	0.97	3.805(5)	2.92	152

[a]Symmetry code: (i) 1−*x*, −*y*, 2−*z*, (ii) 2−*x*, −*y*, 2−*z*, (iii) 1−*x*, 1−*y*, 2−*z*.

Table 4. Selected Bond Distances and Angles and Geometrical Parameters for C−H···X Intermolecular Interactions in 2c (Å, deg)

bond distances		bond angles	
P1−C1	1.835(3)	C1−P1−C4	95.6(1)
P1−C4	1.821(4)	C1−P1−C6	96.8(2)
P1−C6	1.834(5)	C4−P1−C6	97.4(2)
O1−C8	1.180(4)		
O2−C8	1.327(4)		
O2−C9	1.464(6)		

	intermolecular interactions[a]			
	D−H	D···A	H···A	D-H···A
C1−H···F3	0.97	3.429(5)	2.50	160
C3−H···F2	0.97	3.598(6)	2.65	164
C6−H···F4	0.97	3.569(6)	2.66	156
C2−H···O1^{i}	0.97	3.233(5)	2.44	138
C3−H···F1^{ii}	0.97	3.146(4)	2.33	141
C6−H···F1^{iii}	0.97	3.438(5)	2.57	148
C5−H···F3^{iii}	0.97	3.524(7)	2.57	169
C4−H···F5^{iv}	0.97	3.515(5)	2.56	167

[a]Symmetry code: (i) 1−*x*, −*y*, 1−*z*., (ii) −*x*, 1−*y*, 1−*z*, (iii) *x*+1/2, 1/2−*y*, *z*+1/2, (iv) −*x*, −*y*, 1−*z*.

(CH_3), 47.5 (d, $^1J_{PC}$ = 20.6 Hz, 2C, NCH_2P), 55.2 (d, $^1J_{PC}$ = 34.4 Hz, 1C, N^+CH_2P), 60.7 (1C, N^+CH_2CO), 63.8 (1C, CH_2CH_3), 71.3 (1C, NCH_2N), 82.1 (2C, NCH_2N^+), 165.4 (1C, COOEt). ESI-MS: observed *m*/*z* 244, calculated 244 per $C_{10}H_{19}N_3O_2P$ $[M - PF_6]^+$. $S_{25\,°C}$ (H_2O): 1.9 g L^{-1}.

Synthesis of *cis*-[(PTACH$_2$COOEt)$_2$PtBr$_2$]Br$_2$, 2aPt. *cis*-$[PtBr_2(PTA)_2]$ (0.15 g, 2.24 × 10^{-4} mol) was suspended in MeOH (30 mL), and a large excess of $BrCH_2COOEt$ (500 μL = 0.75 g, 4.48 × 10^{-3} mol, 20 equiv) was added. The mixture was stirred overnight at room temperature and then taken to dryness, leaving a white residue, which was washed with MeOH (0.119 g, 1.43 × 10^{-4} mol, yield 64%). $^{31}P\{^1H\}$NMR (121.5 MHz, CD_3OD): δ −42.12 ppm (br s, $^1J_{PtP}$ 3364 Hz). ^1H NMR (300 MHz, CD_3OD) δ (ppm): 1.35 (t, $^3J_{HH}$ = 5 Hz, 3H, CH_2CH_3), 4.20 (s, 2H, N^+CH_2CO), 4.32 (q, $^3J_{HH}$ = 5 Hz, 2H, CH_2), 4.50 (d, $^2J_{HH}$ = 11 Hz, 1H, NCH_2N), 4.67 (d, $^2J_{HH}$ = 11 Hz, 1H,

dx.doi.org/10.1021/ic402953s | Inorg. Chem. 2014, 53, 4881−4890

NCH_2N), 4.80−5.00 (m, 4H, N^+CH_2P + NCH_2P), 5.15 (d, 2H, $^2J_{HH}$ = 9 Hz) 5.45 (d, 2H, $^2J_{HH}$ = 9 Hz, N^+CH_2N).

Synthesis of *cis*-[$(PTACH_2COOEt)_2PtCl_2$]Cl_2, 2bPt. The ligand ($PTACH_2COOEt$)Cl (0.112 g, 4 × 10^{-4} mol, 2 equiv) was dissolved in 1.5 mL of water, and this solution was added to a second one obtained by dissolving K_2PtCl_4 (0.083 g, 2 × 10^{-4} mol, 1 equiv) in 0.7 mL of water. A white precipitate was formed immediately. After 30 min under stirring, the solid was separated by centrifugation, washed with water (2 × 2 mL), and dried under vacuum over P_2O_5 (0.135 g, 1.6. 10^{-4} mol, yield 80%). Anal. Calcd for $C_{20}H_{38}Cl_4N_6O_4P_2Pt$ (MW 825): C 29.1, H 4.6, N 10.2. Found: C 28.7, H 4.9, N 9.7. IR: CO 1746 cm^{-1}. $^{31}P\{^1H\}$ NMR (121.5 MHz, d_6-dmso) δ (ppm): −38.87 (s, $^1J_{PtP}$ 3489 Hz). ^1H NMR (300 MHz, d_6-dmso) δ (ppm): 1.22 (t, $^3J_{HH}$ = 5 Hz, 3H, $-CH_2CH_3$), 4.20 (m, 4H, NCH_2P + 2H N^+CH_2CO), 4.32 (q, $^3J_{HH}$ = 5 Hz, 2H, $-CH_2CH_3$), 4.40−4.70 (m, 4H), 5.00−5.30 (m, 4H). $S_{25\ °C}$ (H_2O): 0.7 g L^{-1}. The aqueous supernatant was examined by $^{31}P\{^1H\}$ NMR, and the singlet with satellites of Pt complex (−38.9 s, $^1J_{PtP}$ = 3511 Hz) was the only observed signal.

Synthesis of [$CpRu(PPh_3)(PTACH_2COOEt)Cl$]Cl, 2bRu. *Method 1.* To a solution of [$CpRu(PPh_3)(PTA)Cl$] (0.1 g, 0.16 × 10^{-3} mol) in 20 mL of acetone was added dropwise a 5-fold excess of ethyl chloroacetate (0.099 g, 0.8 × 10^{-3} mol). The complete conversion into the final product required 20 h at room temperature. The volume was reduced to 1 mL, and the addition of diethyl ether gave a yellow precipitate of **2bRu**, which was filtered and washed with ether (0.1 g, 0.13 × 10^{-3} mol, yield 81%).

Method 2. A slight excess of solid ($PTACH_2COOEt$)Cl (**2b**) (0.06 g, 0.2 × 10^{-3} mol, 1.5 equiv) was added under stirring to a solution of [$CpRu(PPh_3)_2Cl$] (0.1 g, 0.14 × 10^{-3} mol) in 30 mL of acetone. The mixture was refluxed for 6 h. The evaporation of the solvent to a small volume and the slow addition of diethyl ether gave a yellow precipitate of **2bRu**, which was filtered and dried in air (0.05 g, 0.75 × 10^{-3} mol, yield 54%). Anal. Calcd for $C_{33}H_{39}Cl_2N_3O_2P_3Ru$ (MW 743): C 53.3, H 5.3, N 5.6. Found: C 54.3, H 4.9, N 5.0. IR: CO 1750 cm^{-1}. $^{31}P\{^1H\}$ NMR (121.5 MHz, $CDCl_3$) δ (ppm): 46.32 (d, PPh_3, $^2J_{PP}$ = 43.7 Hz), −14.38 (d, **2**, $^2J_{PP}$ = 43.7 Hz). ^1H NMR (300 MHz, d_6-dmso): 1.35 (t, 3H, OCH_2CH_3, $^2J_{HH}$ = 11 Hz), 2.70 (m, 2H, $-NCH_2COOEt$), 3.2−4.0 (br m, 4H, cage), 4.18 (q, 2H, OCH_2CH_3, $^2J_{HH}$ = 11 Hz), 4.35 (m, 4H, cage), 4.56 (s, 5H, Cp), 4.8−5.0 (m, 4H, N^+CH_2N), 7.35−7.45 (15H, PPh_3). $^{13}C\{^1H\}$ NMR (300 MHz, $CDCl_3$) δ (ppm): 14.1 (s, CH_3), 49.5 (d, NCH_2P, $^1J_{PC}$ = 20.1 Hz), 51.6 (d, N^+CH_2P, $^1J_{PC}$ = 32.0 Hz), 57.2 (s N^+CH_2COOEt), 60.0 (s OCH_2CH_3), 65.5 (s, NCH_2N), 79.4 (s, Cp), 79.8 (s, N^+CH_2N), 137−128 (18H, aromatic), 169.0 (s, 1C, CO). ESI-MS: observed *m/z* 708, calculated 708 for $C_{33}H_{39}ClN_3O_2P_2Ru$ [M − Cl]$^+$. $S_{25\ °C}$ (H_2O): 21.5 g L^{-1}.

Synthesis of ($PTACH_2CH_2COOEt$)Br, 3a. A solution of PTA (0.200 g, 1.3 ·10^{-3} mol) in 30 mL of acetone was treated with ethyl 3-bromopropionate (400 μL, 0.56 g, 3.1 × 10^{-3} mol, 2.4 equiv) and stirred at room temperature for 48 h. The white precipitate was filtered off and washed with acetone (2 × 2 mL) (0.27 g, 8 × 10^{-4} mol, 63%). Anal. Calcd for $C_{11}H_{21}BrN_3O_2P$ (MW 338): C 39.1, H 6.2, N 12.4. Found: C 40.3, H 6.2, N 11.9. $^{31}P\{^1H\}$ NMR (121.5 MHz, CD_3OD) δ (ppm): −82.67 (s). ^1H NMR (300 MHz, CD_3OD) δ (ppm): 1.25 (t, $^3J_{HH}$ = 8 Hz, 3H, CH_3), 2.95 (t, 2H, $N^+CH_2CH_2CO$), 3.22 (t, 2H, $N^+CH_2CH_2CO$), 3.9 (m, 4H, NCH_2P), 4.2 (q, $^3J_{HH}$ = 8 Hz, 2H, Et + d, $^3J_{HP}$ = 5.6 Hz 2H, N^+CH_2P), 4.45 (d, $^2J_{HH}$ = 12 Hz 1 H, NCH_2N), 4.6 (d, $^2J_{HH}$ = 12 Hz, 1H, NCH_2N), 4.90 (d, $^2J_{HH}$ = 11 Hz, 2H, N^+CH_2N), 5.10 (d, $^2J_{HH}$ = 11 Hz, 2H, N^+CH_2N). ESI-MS: observed *m/z* 258, calculated 258 for $C_{11}H_{21}N_3O_2P$ [M − Br]$^+$. $S_{25\ °C}$ (H_2O): 173 g L^{-1}.

Synthesis of ($PTACH_2CH_2COOEt$)PF_6, 3c. ($PTACH_2CH_2COOEt$)PF_6 was obtained by adding a solution of KPF_6 (0.28 g, 1.5 × 10^{-3} mol) in 1 mL of methanol to a solution of ($PTACH_2CH_2COOEt$)Br (0.52 g, 1.5 × 10^{-3} mol) in 20 mL of methanol. The solution was stirred at room temperature for 10 min and then slowly concentrated under nitrogen, giving a white solid, which was filtered off and washed with methanol (0.27 g, 7 × 10^{-4} mol, yield 47%). Anal. Calcd for $C_{11}H_{21}F_6N_3O_2P_2$ (MW 403): C 32.8, H 5.2, N 10.4. Found: C 33.2, H 5.4, N 10.2. IR: CO 1746 cm^{-1}. $^{31}P\{^1H\}$ NMR (121.5 MHz, d_6-dmso) δ (ppm): −85.08 s, −143.2 sept ($^1J_{FP}$ 707 Hz). ^1H NMR (300 MHz, d_6-dmso) δ (ppm): 1.20 (t, $^3J_{HH}$ = 9 Hz, 3H, CH_3), 2.90 (t, 2H, $N^+CH_2CH_2CO$), 3.07 (t, 2H, $N^+CH_2CH_2CO$), 3.82 (m, 4H, NCH_2P), 4.10 (q, $^3J_{HH}$ = 9 Hz, 2H, Et) 4.31 (m, 2H, N^+CH_2P + 1 H, NCH_2N), 4.48 (d, $^2J_{HH}$ = 11 Hz, 1H, NCH_2N), 4.80 (d, $^2J_{HH}$ = 11 Hz, 2H, N^+CH_2N), 4.95 (d, $^2J_{HH}$ = 11 Hz, 2H, N^+CH_2N). $^{13}C\{^1H\}$ NMR (100.57 MHz, CD_3OD) δ (ppm): 14.4 (CH_3), 26.1 ($CH_2CH_2N^+$), 47.4 (d, $^1J_{PC}$ 21.4 Hz, 2C, NCH_2P), 54.1 (d, $^1J_{PC}$ 34.5 Hz, 1C, N^+CH_2P), 58.6 (1C, CH_2CH_2CO), 62.5 (1C, CH_2CH_3), 71.2 (1C, NCH_2N), 82.2 (2C, NCH_2N^+), 171.3 (1C, COOEt). ESI-MS: observed *m/z* 258, calculated 258 for $C_{11}H_{21}N_3O_2P$ [M − PF_6]$^+$. $S_{25\ °C}$ (H_2O): 1.6 g L^{-1}.

Synthesis of *cis*-[$(PTACH_2CH_2COOEt)_2PtCl_2$]$(PF_6)_2$, 3cPt. The ligand ($PTACH_2CH_2COOEt$)$PF_6$, **3c** (0.080 g, 2. 10^{-4} mol, 2 equiv), was dissolved in 2 mL of water, and this solution was added to a second one obtained by dissolving K_2PtCl_4 (0.041 g, 1 × 10^{-4} mol, 1 equiv) in 1 mL of water. The milky suspension was stirred for 18 h, and then a white solid was separated by centrifugation, washed with water (2 × 2 mL), and dried under vacuum over P_2O_5 (0.061 g, 0.5 × 10^{-4} mol, yield 57%). Anal. Calcd for $C_{22}H_{42}Cl_2F_{12}N_6O_4P_4Pt.H_2O$ (MW 1090): C 24.6, H 3.9, N 7.8. Found: C 24.2, H 4.0, N 7.7. IR: CO 1748 cm^{-1}. $^{31}P\{^1H\}$ NMR (121.5 MHz, d_6-dmso) δ (ppm): −41.69 (s, $^1J_{PtP}$ = 3425 Hz), −143.25 (PF_6^-, $^1J_{FP}$ = 707 Hz). ^1H NMR (300 MHz, d_6-dmso) δ (ppm): 1.20 (t, $^3J_{HH}$ = 9 Hz, 3H, CH_3), 2.95 (m, 2H, $N^+CH_2CH_2CO$), 3.4 (m, 6H, NCH_2P + $N^+CH_2CH_2CO$), 4.10 (q, $^3J_{HH}$ = 9 Hz, 2H, CH_2CH_3), 4.5 (m, 4H, N^+CH_2P + NCH_2N), 5.0 (m, 4H, N^+CH_2N). $S_{25\ °C}$ (H_2O): 0.02 g L^{-1}.

Synthesis of [$CpRu(PPh_3)(PTACH_2CH_2COOEt)Cl$]$PF_6$, 3cRu. A slight excess of solid **3c** (0.061 g, 0.15 × 10^{-3} mol, 1.1 equiv) was added under stirring to a solution of [$CpRu(PPh_3)_2Cl$], (0.10 g, 0.14 × 10^{-3} mol) in acetone (25 mL), and the mixture was refluxed for 4 h. The solvent was then removed in vacuo, leaving an orange solid, which was washed with diethyl ether, then filtered and dried in air (0.11 g, 0.12 × 10^{-3} mol, yield 88%). Anal. Calcd for $C_{34}H_{41}ClF_6N_3O_2P_3Ru$ (MW 866.7): C 47.1, H 4.8, N 4.9. Found: C 45.1, H 4.6, N 4.9. IR: CO 1750 cm^{-1}. $^{31}P\{^1H\}$ NMR (121.5 MHz, CD_3OD) δ (ppm): 45.55 (d, PPh_3, $^2J_{PP}$ = 43.7 Hz), −14.55 (d, **3c**, $^2J_{PP}$ = 43.7 Hz), −143.25 (PF_6^-, $^1J_{FP}$ = 707 Hz). ^1H NMR (300 MHz, CD_3OD) δ (ppm): 1.29 (t, $^3J_{HH}$ = 11 Hz, 3H, OCH_2CH_3), 2.63 (br s, 2H, $N^+CH_2CH_2COOEt$), 3.2−4.0 (br m, 6H), 4.18 (q, $^3J_{HH}$ = 11 Hz, 2H, OCH_2CH_3), 4.35 (m, 4H), 4.55 (s, Cp, 5H), 4.6−4.8 (m, 4H, N^+CH_2N), 7.35−7.50 (15H, PPh_3). $^{13}C\{^1H\}$ NMR (300 MHz, CD_3OD) δ (ppm): 14.0 (s, OCH_2CH_3), 42.5 (d, NCH_2P, $^1J_{PC}$ = 20.0 Hz), 52.0 (d, N^+CH_2P, $^1J_{PC}$ = 32.0 Hz), 56.1 (s, $N^+CH_2CH_2CO_2Et$), 59.9 (s, $N^+CH_2CH_2CO_2Et$), 60.6 (s, OCH_2CH_3), 64.5 (s, NCH_2N), 80.1 (s, Cp), 80.8 (s, N^+CH_2N), 137−127 (aromatics), 170.03 (s, CO). ESI-MS: observed *m/z* 722, calculated 722 for $C_{34}H_{41}ClN_3O_2P_2Ru$ [M − PF_6]$^+$.

Crystallography. The crystallographic data for **1d**, **1cRu**, and **2c** were collected on a Nonius Kappa CCD diffractometer at room temperature using graphite-monochromated Mo Kα radiation (λ = 0.71073 Å). Data sets were corrected for Lorentz−polarization effects; data for **1cRu** were corrected also for absorption effects.[13] The crystal parameters and other experimental details of the data collections are summarized in Table 1.

The structures were solved by direct methods (SIR97)[14] and refined by full-matrix least-squares methods with all non-hydrogen atoms anisotropic. Hydrogens were included on calculated positions, riding on their carrier atoms. In **1d**, a case of substitutional disorder, i.e., a situation in which the same site in two unit cells is occupied by different types of atoms, was present, involving atoms P1 and N3. The positions of the two atoms were assigned on the basis of the highest SOF.

All calculations were performed using SHELXL-97[15] implemented in the WINGX system of programs.[16] Selected bond distances and angles and geometrical parameters for C−H···X and C−H···π interactions for **1d**, **1cRu**, and **2c** are given in Tables 2, 3, and 4. We have considered only contacts where C−H···X angles are greater than 130° and H···X distances are shorter than the sum of the van der Waals radii.

dx.doi.org/10.1021/ic402953s | Inorg. Chem. 2014, 53, 4881−4890

ORTEP III[17] views of **1d**, **1cRu**, and **2c** are given in Figures 1, 2, and 3.

Growth Inhibition Assays. Cell growth inhibition assays were carried out using the leukemia cell line K562 and two human ovarian cancer cell lines, A2780 and SKOV3; A2780 cells are cisplatin-sensitive, and SKOV3 cells are cisplatin-resistant. Cell lines were obtained from ATCC (Manassas, VA, USA) and maintained in RPMI 1640, supplemented with 10% fetal bovine serum (FBS), penicillin (100 U mL^{-1}), streptomycin (100 U mL^{-1}), and glutamine (2 mM); the pH of the medium was 7.2 and incubation was performed at 37 °C in a 5% CO_2 atmosphere. Cells were routinely passaged every 3 days at 70% confluence; for the adherent cell lines, 0.05% trypsin-EDTA (Lonza) was used. The antiproliferative activity of compounds was tested with the MTT assay. The cells were seeded in triplicate in 96-well trays at a density of 5×10^3 in 50 μL of complete medium. Stock solutions (20 mM) of each compound were made in dmso and diluted in complete medium to give final concentrations of 0.1, 1, 10, 50, and 100 μM. Cisplatin was employed as a control for the cisplatin-sensitive A2780 cell line and for the cisplatin-resistant SKOV3. Untreated cells were placed in every plate as a negative control. The cells were exposed to the compounds, in 100 μL total volume, for 72 h, and then 25 μL of a 12 mM solution of 3-(4,5-dimethylthiozol-2-yl)-2,5-diphenyltetrazolium bromide solution (MTT) was added. After 2 h of incubation, 100 μL of lysing buffer (50% DMF + 20% SDS, pH 4.7) was added to convert the MTT solution into a violet-colored formazan. After an additional 18 h the solution absorbance, proportional to the number of live cells, was measured by spectrophotometer at 570 nm and converted into % of growth inhibition.[18]

RESULTS AND DISCUSSION

The new ligands, as halides salts **1X** (**1a**, X = Br and **1b**, X = I), **2X** (**2a**, X = Br and **2b**, X = Cl), and **3X** (**3a**, X = Br), can be easily prepared in a pure form because the N-alkylation of PTA is a selective process giving exclusively monoalkylated cationic derivatives, as previously reported for many PTA derivatives including MePTA[19] and larger and more functionalized products.[20] In general, the N-alkylation of PTA can be performed with either alkyl bromides or alkyl iodides, but the reaction is faster with iodide. When the alkylating agent bears the halide on an activated carbon atom (benzylic, allylic, or α to a carbonylic group), the reaction is faster and takes place also with chloro derivatives.[21] The alkylation of PTA is generally carried out in acetone and occurs with product precipitation, which probably drives the process nearly to completeness giving fairly pure products.

Synthesis and Characterization of 1a–d and Coordination to Pt(II) and Ru(II). The ligand **1a** was obtained in two steps starting from 2-bromoethanol, which was first acetylated with acetic anhydride, and the resulting bromoester was then used as an alkylating agent for PTA. The iodide **1b** was obtained in the same way from 2-iodoethanol (Scheme 2). The alkylation step is faster with the alkyl iodide, but the ^{31}P NMR observation of the solution shows the formation of P-oxidated impurities, which reduce the yield of **1b**.

The ^{31}P NMR signal, observed at −100 ppm for free PTA in dmso, in the products is shifted to −84.77 ppm (**1a**) or −83.67 ppm (**1b**), close to the values previously reported for other *N*-alkylPTA derivatives.[19−21] In ^1H NMR, the conversion of PTA into an alkyl derivative is typically characterized by an increased number of signals due to the loss of symmetry of the phosphaadamantane cage. Some signals of **1a** and **1b** appear complicated by the geminal coupling between the two diastereotopic protons of each CH_2 group and, for P-bonded CH_2, also by the coupling to that nucleus.

The $[M - Br]^+$ peak of **1a** is observed by ESI-MS at the expected value of 244.

In view of the coordination of ligand **1X** to metal ions, noncoordinating anions are preferred in order to avoid exchange with metal ligands (e.g., metal-bonded chloride), so the bromide of **1a** was exchanged with PF_6^- and with BPh_4^-, giving **1c** and **1d**, respectively.

The solubility in water at 25 °C, remarkable for **1a** (700 g/L), decreases with the increase in the anion size (**1a** = 700 g/L and **1b** = 270 g/L, **1c** = 0.74 g/L and **1d** = 1.56×10^{-2} g/L).

The tetraphenylborate **1d**, recrystallized with acetone and diethyl ether, gave crystals suitable for X-ray determination of crystal structure (Figure 1 and Table 2).

The asymmetric unit of **1d** consists of $PTAC_2H_4OCOMe^+$ and BPh_4^- ions; the substitutional disorder, described in the experimental paragraph, makes the P1−C distances abnormally short (Table 2) and the N3−C quite long (N−C mean distance = 1.59[6] Å). Besides electrostatic forces between anions and cations, in this structure, given the absence of "good" proton donors, the different units interact with each other through weak C−H···O hydrogen bonds and through C−H··· π interactions (see Table 2).

The reaction of **1c** with K_2PtCl_4 (molar ratio 2:1) in water (Scheme 3) gave a single complex, *cis*-$[PtCl_2(PTAC_2H_4OCOMe)_2](PF_6)_2$ (**1cPt**), as a precipitate with low solubility in water ($S_{25\ °C}(H_2O)$ = 0.01 g L^{-1}). It was identified by ^{31}P NMR (−41.74 broad singlet, $^1J_{PtP}$ 3495 Hz, in dmso), where the observed shift of the Pt complex signal at −41.74 ppm is about 40 ppm downfield with respect to the free ligand **1c** (−83.33 ppm) and about 10 ppm downfield with respect to the neutral PTA complex *cis*-$[PtCl_2(PTA)_2]$ (^{31}P −51.85 ppm $^1J_{PtP}$ 3285 Hz). These data comply with those found for other Pt complexes of *N*-alkylPTA ligands, e.g., *cis*-$[PtCl_2(MePTA)_2](PF_6)_2$ (^{31}P −43.51 ppm, $^1J_{PtP}$ 3384 Hz)[7b] compared with $MePTAPF_6$ (^{31}P −84.2 ppm).

The broadness observed for the ^{31}P NMR signal of **1cPt** has been reported in many cases for metal complexes of PTA or PTA derivatives by us[7b] and others.[7c−e,8a] We did some additional NMR experiments on **1cPt** in DMSO, and we found that the line broadening is not effected by concentration (the line width does not change by reducing the concentration to 1/10) or temperature (from 25 to 120 °C). Also, on replacing DMSO with DMF the signal does not become sharp.

Scheme 2

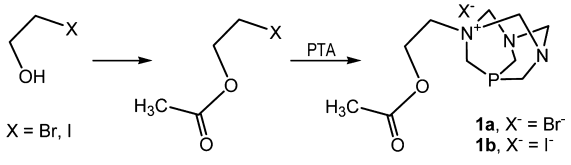

Scheme 3

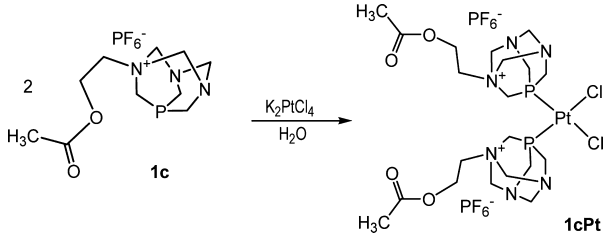

dx.doi.org/10.1021/ic402953s | Inorg. Chem. 2014, 53, 4881−4890

Scheme 4

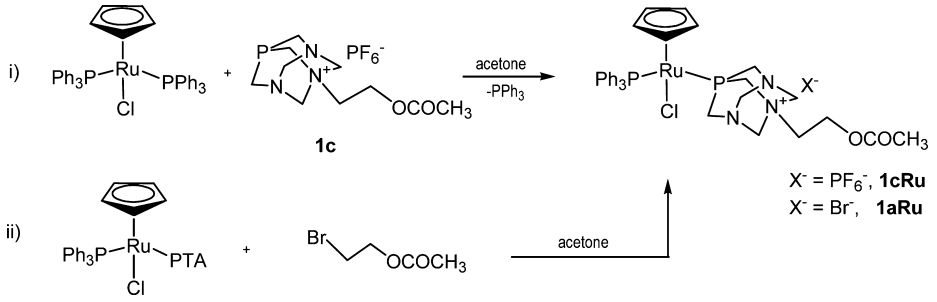

The signal broadening in complex **1cPt** (and analogues) could be the consequence of a restricted conformational freedom around P−Pt bonds due to the presence of two ligands bearing two positive charges, which tend to keep as far as possible one from each other in order to minimize the electrostatic repulsion. The steric hindrance of the alkyl substituents on two spatially close nitrogen atoms could also limit the rotation.

To support this hypothesis, it is useful to verify if in the ^{31}P NMR of a Pt complex bearing only one **1c** ligand the signal is sharp; so we did the following NMR experiment: the known complex $[terpyPt(H_2O)]^{2+}$ was dissolved in DMSO and 1 equiv of ligand **1c** was added to give $[terpyPt(\mathbf{1c})]^{2+}$. After 18 h the observed ^{31}P NMR spectrum was indeed a sharp singlet with satellites at −50.8 with $^1J_{PtP}$ = 3599 Hz.

The isotopic pattern for the $[M - 2PF_6]^{2+}$ ion of **1cPt**, observed by ESI-MS at 377 *m*/*z*, compared with the calculated one, confirmed the composition of the Pt complex, while the value of the PtP coupling constant (3495 Hz) indicates the cis geometry.

The Ru(II) coordination of ligand **1c** was also successfully achieved. This result is particularly relevant because the development of Ru-based drugs is one of the most promising frontiers of research in inorganic medicinal chemistry.[1a,22] For example, the peculiar pharmacological activity of $[RuCl_2(\eta^6\text{-arene})(PTA)]$ (arene = *p*-cymene, toluene, benzene, benzo-15-crown-5, 1-ethylbenzene-2,3-dimethylimidazolium tetrafluoroborate, ethyl benzoate, hexamethylbenzene) complexes, abbreviated RAPTA, was evaluated in mice, and it was observed that they can reduce the growth of lung metastases without action on the primary tumor growth.[23]

Since in our previous work on Ru-containing complexes we found that the combination of PTA and PPh_3 in the same complex seems to improve the antiproliferative activity with respect to single-phosphine analogues,[24] the mixed phosphine complexes $[RuCpCl(PTAC_2H_4OCOMe)(PPh_3)]X$ (X = Br, **1aRu**; X = PF_6^-, **1cRu**) looked like the best candidates for achieving anticancer activity.

Complex **1cRu** was prepared by replacing one PPh_3 of $[RuCpCl(PPh_3)_2]$ with ligand **1c** (Scheme 4, route (i)), while the bromide **1aRu** was obtained by alkylation of the Ru-coordinated PTA in $[RuCpCl(PTA)(PPh_3)]$[25] (Scheme 4, route (ii)).

The first route gives the pure product **1cRu** as a yellow precipitate with a good yield (80%) after 3 h of reflux in acetone. The second requires 24 h at room temperature, and the yield is low (ca. 30%).

In general, the alkylation of metal-bonded PTA seems to occur as a slow process (24 h) when PTA is coordinated to Ru. Attempts to accelerate the reaction by increasing the temperature led to several unidentified side products. In particular, the MePTA complex $[RuCpCl(MePTA)(PPh_3)]PF_6$ (d, 16.06, d, 46.31, $^2J_{PP}$ = 43.7 Hz in dmso) was occasionally observed as a side-product when reaction mixtures were refluxed, probably due to the presence of traces of water. It was previously observed that MePTA is formed by C*α*−C*β* bond breaking of *N*-alkylPTA derivatives in the presence of water.[7c]

We attempted to prepare also Pt complexes of **1a** and **1b** by alkylation of Pt-coordinated PTA, but the product signal was not observed by ^{31}P NMR over 3 days. After prolonged reaction time, signals of P-containing oxidative degradation products started to appear in the ^{31}P NMR.

The ^{31}P NMR spectrum of $[RuCpCl(PTAC_2H_4OCOMe)(PPh_3)]X$ (**1cRu**, X = PF_6; **1aRu**, X = Br) shows two doublets at about 46.5 ppm (Ru-coordinated PPh_3) and −14.5 ppm (Ru-coordinated ligand **1**) reciprocally coupled with $^2J_{PP}$ = 43.7 Hz. These signals are clearly distinguishable from the corresponding ones of the reagent complexes $[RuCpCl(PPh_3)_2]$ for route (i) (38.8 ppm)[26] and $[RuCpCl(PTA)(PPh_3)]$[12] for route (ii) (48.16 and −34.96 ppm, $^2J_{PP}$ = 34.7 Hz).

The solubility in water of **1c** ($S_{25\,°C}$ 0.74 g L^{-1}) decreases upon coordination to Pt (**1cPt**, $S_{25\,°C}$ 0.01 g L^{-1}) and to Ru (**1cRu**, $S_{25\,°C}$ 0.05 g L^{-1}).

Complex **1cRu** was separated in a pure form by recrystallization with acetone and Et_2O, which gave crystals suitable for X-ray diffraction (Figure 2, Table 3).

The asymmetric unit is formed by one Ru complex and one PF_6 anion (not shown in Figure 2). The ruthenium atom is in an octahedral environment since it is bound to a cyclopentadienyl ring (formally three *fac* positions), two phosphorus atoms, one from a triphenylphosphine and one from ligand **1**, and a chloride ion. The coordination geometry of the complex is that of a three-legged "piano stool". For comparative reasons, five structures[27,12] strictly related to the present Ru complex, in which the metal ion is surrounded by PTA, Cl, TriP, and Cp ligands, were retrieved from the Cambridge Crystallographic Database.[28] In these structures the Ru−P(PTA), Ru−P(TriP), Ru-Cp(centroid), and Ru−Cl distances vary in the ranges 2.280−2.314, 2.270−2.309, 1.837−1.890, and 2.449−2.466 Å, respectively, perfectly in line with the structural parameters listed in Table 3.

In the crystal anions and cations are linked not only via electrostatic forces but also by a number of weak C−H···Halide interactions, listed in Table 3.

Synthesis and Characterization of 2a−c and Coordination to Pt(II) and Ru(II). Ligand **2** was prepared as the ethyl esters **2X** (**2a**, X = Br and **2b**, X = Cl) by treating PTA with commercial XCH_2COOEt in acetone. A similar synthesis for the methyl esters $(PTACH_2COOMe)X$ (X = Br and X = Cl) has been reported by Laguna.[21,29]

dx.doi.org/10.1021/ic402953s | *Inorg. Chem.* 2014, 53, 4881−4890

Scheme 5

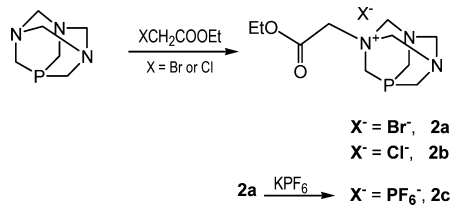

By exchange with KPF_6 in methanol, the bromide **2a** was converted in the PF_6^- salt **2c**, whose X-ray crystal structure was determined (Figure 3, Table 4). The crystal structures of the analogue methyl ester bromide[21] and triflate[29] were previously reported.

In **2c** the asymmetric unit contains the PTA derivative and its counterion; the different units interact with each other through weak C−H···O/F hydrogen bonds.

The reaction of the chloride **2b** with K_2PtCl_4 in water gave the Pt complex *cis*-$[PtCl_2(PTACH_2COOEt)_2]Cl_2$, **2bPt**, characterized by a ^{31}P NMR single signal at −38.87 ppm with $^1J_{PtP}$ = 3489 Hz, confirming the cis geometry.

The bromide analogue of this complex, *cis*-$[PtBr_2(PTACH_2COOEt)_2]Br_2$, **2aPt**, can be obtained by alkylation of Pt-coordinated PTA in *cis*-$[PtBr_2(PTA)_2]$ with $BrCH_2COOEt$ (Scheme 6). The alkylation of PTA bonded to Pt has not been observed before, and it does not occur with the corresponding chloride $ClCH_2COOEt$.

Scheme 6

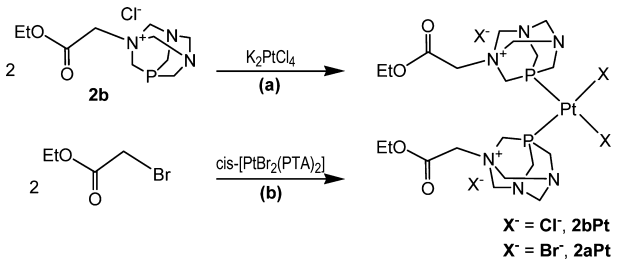

The ruthenium complex $[CpRu(PPh_3)(PTACH_2COOEt)Cl]Cl$, **2bRu**, was prepared either by alkylation of Ru-coordinated PTA in $[CpRu(PPh_3)(PTA)Cl]$ or by substitution of PPh_3 with **2b** in $[CpRu(PPh_3)_2Cl]$, as above-mentioned for the Ru complexes of ligand **1a** and **1c**.

As previously observed for ligand **1X**, the water solubility of **2X** changes with the anion **X** and the trend is $Cl^- > Br^- > PF_6^-$: **2b** ($S_{25\ °C}$ 910 g L^{-1}) > **2a** ($S_{25\ °C}$ 625g L^{-1}) >**2c** ($S_{25\ °C}$ 1.9 g L^{-1}). Although in general we found that the water solubility of these ligands greatly decreases upon coordination, complexes **2bPt** ($S_{25\ °C}$ 0.7 g L^{-1}) and **2bRu** ($S_{25\ °C}$ 21.5 g L^{-1}), where X = Cl^-, maintain some aqueous solubility.

Synthesis and Characterization of 3a and 3c and Coordination to Pt(II) and Ru(II). Ligand **3X**, the superior homologue of **2X**, was also prepared, in order to complete a series of molecules where the distance between the carbonyl carbon and the quaternary nitrogen N^+ is four bonds (**1X**), three bonds (**3X**), and two bonds (**2X**) (Scheme 7). The availability of the three compounds will be useful for investigating the interactions of ligands and their metal complexes with acetylcholine receptors or cation transporters and establishing a structure−activity relationship. In fact it has been proposed that the affinity of a chemical species with acetylcholine receptors is related to its length.[30]

The reaction between 3-bromoethylpropionate and PTA in acetone produced **3a**, which was collected as a white solid after 20 h. The NMR in CD_3OD confirmed the structure, showing a ^{31}P signal at −82.67 ppm and, in ^1H NMR, two signals at 2.95 and 3.22 ppm due to the alkyl chain CH_2 groups besides the typical signals of the alkylated PTA cage.

The PF_6^- salt **3c** was obtained from the bromide by anion exchange with KPF_6 in methanol (Scheme 8).

Scheme 8

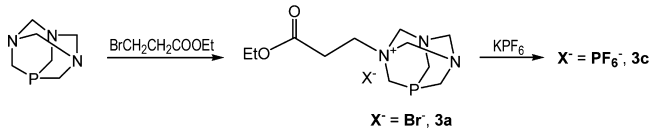

The reaction of **3c** with K_2PtCl_4 in water gave the complex *cis*-$[PtCl_2(PTACH_2CH_2COOEt)_2](PF_6)_2$, **3cPt**, characterized in ^{31}P NMR data by a singlet at −41.69 ppm with a $^1J_{PtP}$ = 3425 Hz.

The Ru complex **3cRu** was also obtained with a good yield from the reaction of $[CpRu(PPh_3)_2Cl]$ with a slight excess of solid **3c** in refluxing acetone. Its ^{31}P NMR in CD_3OD shows two doublets at 45.55 ppm due to coordinated PPh_3 and −14.55 ppm due to Ru-bonded **3c**, reciprocally coupled with $^2J_{PP}$= 43.7 Hz.

Antiproliferative Activity of 1c, 2b, 2c, 3c, 1cPt, 1cRu, 2bPt, 2cRu, and 3cPt. The antiproliferative activity of ligands **1c**, **2b**, **2c**, and **3c** and complexes **1cPt**, **1cRu**, **2bPt**, **2cRu**, and **3cPt** was tested on two human ovarian cancer cell lines, A2780 and SKOV3, and on the leukemic line K562, in comparison with cisplatin, and the results are reported in Table 5.

The complexes to test were designed and chosen in order to get the highest activity on the basis of previously reported characteristics, e.g., cis geometry for Pt complexes, Ru state of oxidation = 2, and chloride as metal-bonded halide (rather than bromide and iodide). Moreover all complexes tested have Cl^- or PF_6^- as counterions so as to avoid ligand exchanges.

These figures indicated that the organic free ligands **1c**, **2b**, **2c**, and **3c** do not show appreciable activity on all three lines, while their metal complexes do in some cases.

The platinum complexes **1cPt**, **2bPt**, and **3cPt** show low activity on cisplatin-resistant SKOV3 and an appreciable activity on cisplatin-sensitive A2780. These data allow us to hypothesize a cisplatin-like action for Pt complexes.

Scheme 7

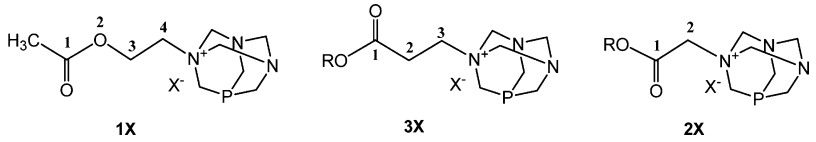

dx.doi.org/10.1021/ic402953s | Inorg. Chem. 2014, 53, 4881−4890

Table 5. Estimated IC_{50} (μM) of 1c, 2b, 2c, 3c, 1cPt, 1cRu, 2bPt, 2cRu, and 3cPt on A2780, SKOV3, and K562 Cell Lines[a]

compound	A2780	SKOV3	K562
1c	49 ± 1	>100	>100
2b	46 ± 3	>100	>100
2c	47 ± 5	>100	>100
3c	56 ± 4	>100	>100
1cPt	18 ± 3	42 ± 11	40 ± 2
1cRu	4.7 ± 1	6.0 ± 0.5	5.1 ± 0.3
2bPt	36 ± 4	47 ± 2	66 ± 3
2bRu	5.8 ± 0.5	8.3 ± 0.8	5.5 ± 0.2
3cPt	17 ± 4	63 ± 2	59 ± 2
cisplatin	0.91 ± 0.08	7.9 ± 3	7.4 ± 1

[a]Results are presented as a mean ± SD of three independent experiments performed in triplicates.

The Ru complexes of **1c** and **2c** have a remarkable activity on all three cell lines. In particular, complex **1cRu** was found very active on all three tested cell lines. This observation is relevant as, in many cases, Ru complexes were found inactive against primary tumors.

CONCLUSION

Three PTA derivatives (**1X**, **2X**, and **3X**), designed as ligands for Pt and Ru therapeutics, as well as their Pt(II) and Ru(II) complexes, were prepared and characterized.

All ligands and their Pt and Ru complexes, as chloride or PF_6^- salts, were tested for antiproliferative activity on three human cancer cell lines, and the best performance was obtained by Ru complexes. The X-ray crystal structure of complex **1cRu** was determined.

These results encourage us to investigate the behavior of all these compounds as neuroactive species: the nontoxic salts **1c**, **2c**, **3c**, and **2b** could interfere with the cholinergic cascade involved in Alzheimer disease, while, after appropriate coordination, they could act as carriers for metal ions through the blood–brain barrier, allowing them to act as metallotherapeutics in the central nervous system.

ASSOCIATED CONTENT

Supporting Information

Crystallographic data in cif format. This material is available free of charge via the Internet at http://pubs.acs.org. Crystallographic data for the structural analysis of **1d**, **2c**, and **1cRu** have been deposited at the Cambridge Crystallographic Data Center, 12 Union Road, Cambridge, CB2 1EZ, UK, and are available free of charge from the Director on request quoting the deposition number CCDC 960858, 960859, and 960860 for **1d**, **2c**, and **1cRu**, respectively.

AUTHOR INFORMATION

Corresponding Author

*E-mail: p.bergamini@unife.it. Tel: +39 0532 455129. Fax: +39 0532 455167.

Notes

The authors declare no competing financial interest.

ACKNOWLEDGMENTS

We thank Dr. T. Bernardi, Dr. E. Bianchini, and Mr. P. Formaglio for technical assistance and CIRCMSB (Consorzio Interuniversitario di Ricerca in Chimica dei Metalli nei Sistemi Biologici) for support.

REFERENCES

(1) (a) Barry, N. P. E.; Sadler, P. J. *Chem. Commun.* **2013**, *49*, 5106–5131. (b) Harper, B. W.; Krause-Heuer, A. M.; Grant, M. P.; Manohar, M.; Garbutcheon-Singh, K. B.; Aldrich-Wright, J. R. *Chem.—Eur. J.* **2010**, *16*, 7064–7077. (c) Wheate, N. J.; Walker, S.; Craig, G. E.; Oun, R. *Dalton Trans.* **2010**, *39*, 8113–8127.

(2) Breydo, L.; Uversky, V. N. *Metallomics* **2011**, *3* (11), 1163–1180.

(3) (a) Jacobs, S.; McCully, C. L.; Murphy, R. F.; Bacher, J.; Balis, E. F. M.; Fox, E. E. *Cancer Chemother. Pharmacol.* **2010**, *65*, 817–824. (b) Bernocchi, G.; Bottone, M. G.; Piccolini, V. M.; Dal Bo, V.; Santin, G.; De Pascali, S. A.; Migoni, D.; Fanizzi, F. P. *Chemother. Res. Pract.* **2011**, 1–14.

(4) (a) Valensin, D.; Gabbiani, C.; Messori, L. *Coord. Chem. Rev.* **2012**, *256*, 2357–2366. (b) Kenche, V. B.; Hung, L. W.; Perez, K.; Volitakes, I.; Ciccotosto, G.; Kwok, J.; Critch, N.; Sherratt, N.; Cortes, M.; Lal, V.; Masters, C. L.; Murakami, K.; Cappai, R.; Adlard, P. A.; Barnham, K. J. *Angew. Chem., Int. Ed.* **2013**, *52*, 3374–3378. (c) Collin, F.; Sasaki, I.; Eury, H.; Faller, P.; Hureau, C. *Chem. Commun.* **2013**, *49*, 2130–2132.

(5) (a) Pardridge, W. M. *Curr. Opin. Pharmacol.* **2006**, *6*, 494–500. (b) Pavan, B.; Dalpiaz, A. *Curr. Pharm. Des.* **2011**, *17*, 3560–3576. (c) Manfredini, S.; Pavan, B.; Vertuani, S.; Scaglianti, M.; Compagnone, D.; Biondi, C.; Scatturin, A.; Manganelli, S.; Ferraro, L.; Prasad, P.; Dalpiaz, A. *J. Med. Chem.* **2002**, *45*, 559–562. (d) Napolitano, C.; Scaglianti, M.; Scalambra, E.; Manfredini, S.; Ferraro, L.; Beggiato, S.; Vertuani, S. *Molecules* **2009**, *14*, 3268–3274.

(6) Koepsell, H.; Schmitt, B. M.; Gorboulev, V. *Rev. Physiol. Biochem. Pharmacol.* **2003**, *150*, 36–90.

(7) (a) Bergamini, P.; Marvelli, L.; Marchi, A.; Bertolasi, V.; Fogagnolo, M.; Formaglio, P.; Sforza, F. *Inorg. Chim. Acta* **2013**, *398*, 11–18. (b) Bergamini, P.; Marvelli, L.; Marchi, A.; Vassanelli, F.; Fogagnolo, M.; Formaglio, P.; Bernardi, T.; Gavioli, R.; Sforza, F. *Inorg. Chim. Acta* **2012**, *391*, 162–170. (c) Kirillov, A. M.; Smolensky, P.; Haukka, M.; Guedes da Silva, M. F. C.; Pombeiro, A. J. L. *Organometallics* **2009**, *28*, 1683–1687. (d) Romerosa, A.; Saoud, M.; Campos-Malpartida, T.; Lidrissi, C.; Serrano-Ruiz, M.; Peruzzini, M.; Garrido, J. A.; García-Maroto, F. *Eur. J. Inorg. Chem.* **2007**, 2803–2812. (e) Porchia, M.; Benettolo, F.; Refosco, F.; Tisato, F.; Marzano, C.; Gandin, V. *J. Inorg. Biochem.* **2009**, *103*, 1644–1651.

(8) (a) Phillips, A. D.; Gonsalvi, L.; Romerosa, A.; Vizza, F.; Peruzzini, M. *Coord. Chem. Rev.* **2004**, *248*, 955–993. (b) Bravo, J.; Bolaño, S.; Gonsalvi, L.; Peruzzini, M. *Coord. Chem. Rev.* **2010**, *254*, 555–607. (c) Guerrero, E.; Miranda, S.; Lüttenberg, S.; Fröhlich, N.; Koenen, J.; Mohr, F.; Cerrada, E.; Laguna, M.; Mendía, A. *Inorg. Chem.* **2013**, *52*, 6635–6647. (d) Serrano-Ruiz, M.; Aguilera-Sáez, L. M.; Lorenzo-Luis, P.; Padrón, J. M.; Romerosa, A. *Dalton Trans.* **2013**, *42*, 11212–11219.

(9) (a) Dyson, P. J.; Sava, G. *Dalton Trans.* **2006**, 1929–1933. (b) Renfrew, A. K.; Juillerat-Jeanneret, L.; Dyson, P. J. *J. Organomet. Chem.* **2011**, *696*, 772–779. (c) Kilpin, K. J.; Cammack, S. M.; Clavel, C. M.; Dyson, P. J. *Dalton Trans.* **2013**, *42*, 2008–2014. (d) Nazarov, A. A.; Hartinger, C. G.; Dyson, P. J. *J. Organomet. Chem.* **2014**, *751*, 251–260. (e) Pettinari, R.; Pettinari, C.; Marchetti, F.; Clavel, C. M.; Scopelliti, R.; Dyson, P. J. *Organometallics* **2013**, *32*, 309–316.

(10) Daigle, D. J.; Decuir, T. J.; Robertson, J. B.; Darensbourg, D. J. *Inorg. Synth.* **1998**, *32*, 40.

(11) Krogstad, D. A.; Cho, J.; DeBoer, A. J.; Klitzke, J. A.; Sanow, W. R.; Williams, H. A.; Halfen, J. A. *Inorg. Chim. Acta* **2006**, *359*, 136–148.

(12) (a) Bruce, M. I.; Wong, F. S.; Skelton, B. W.; White, A. H. *J. Chem. Soc., Dalton Trans.* **198**113981405.

(13) Blessing, R. H. *Acta Crystallogr.* **1995**, *A51*, 33–38.

(14) Altomare, A.; Burla, M. C.; Camalli, M.; Cascarano, G.; Giacovazzo, C.; Guagliardi, A.; Moliterni, A. G.; Polidori, G.; Spagna, R. *J. Appl. Crystallogr.* **1999**, *32*, 115–119.

(15) Sheldrick, G. M. *SHELXL97, Program for Crystal Structure Refinement*; University of Göttingen: Göttingen, Germany, 1997.
(16) Farrugia, L. J. *J. Appl. Crystallogr.* **1999**, *32*, 837−838.
(17) Burnett, M.N.; Johnson, C.K. *ORTEP-III: Oak Ridge Thermal Ellipsoid Plot Program for Crystal Structure Illustrations*; Report ORNL-6895; Oak Ridge National Laboratory: Oak Ridge, TN, 1996.
(18) Hansen, M. B.; Nielsen, S. E.; Berg, K. J. *J. Immunol. Methods* **1989**, *119*, 203−210.
(19) Daigle, D. J.; Pepperman, A. B., Jr. *J. Heterocycl. Chem.* **1975**, *12*, 579−580.
(20) (a) Krogstad, D. A.; Ellis, G. S.; Gunderson, A. K.; Hammrich, A. J.; Rudolf, J. W.; Halfen, J. A. *Polyhedron* **2007**, *26*, 4093. (b) Krogstad, D. A.; Gohmann, K. E.; Sunderland, T. L.; Geis, A. L.; Bergamini, P.; Marvelli, L.; Young, V. G., Jr. *Inorg. Chim. Acta* **2009**, *362*, 3049−3055.
(21) García-Moreno, E.; Cerrada, E.; Bolsa, M. J.; Luquin, A.; Laguna, M. *Eur. J. Inorg. Chem.* **2013**, 2020−2030.
(22) Alessio, E.; Mestroni, G.; Bergamo, A.; Sava, G. *Curr. Top. Med. Chem.* **2004**, *4*, 1525−1535.
(23) Scolaro, C.; Bergamo, A.; Bresciani, L.; Brescacin, L.; Delfino, R.; Cocchietto, M.; Laurenczy, G.; Geldbach, T. J.; Sava, G.; Dyson, P. J. *J. Med. Chem.* **2005**, *48*, 4161−4171.
(24) Hajji, L.; Saraiba-Bello, C.; Romerosa, A.; Segovia-Torrente, G.; Serrano-Ruiz, M.; Bergamini, P.; Canella, A. *Inorg. Chem.* **2011**, *50*, 873−882.
(25) García-Fernández, A.; Díez, J.; Gamasa, M. P.; Lastra, E. *Inorg. Chem.* **2009**, *48*, 2471−2481.
(26) Consiglio, G.; Morandini, F.; Bangerter, F. *Inorg. Chem.* **1982**, *21*, 455−457.
(27) (a) Romerosa, A.; Campos-Malpartida, T.; Lidrissi, C.; Saoud, M.; Serrano-Ruiz, M.; Peruzzini, M.; Garrido-Cardenas, J. A.; Garcia-Maroto, F. *Inorg. Chem.* **2006**, *45*, 1289−1298. (b) Nair, R. P.; Kim, T. H.; Frost, B. J. *Organometallics* **2009**, *28*, 4681−4688.
(28) Allen, F. H. *Acta Crystallogr.* **2002**, *B58*, 380−388.
(29) Schäfer, S.; Frey, W.; Hashmi, A. S. K.; Cmrecki, V.; Luquin, A.; Laguna, M. *Polyhedron* **2010**, *29*, 1925−1932.
(30) Ing, H. R. *Science* **1949**, *109*, 264−266.